Toward Optimal Secondary Furnace Heat Exchanger: Acquisition of Heat Transfer Correlations

Simon Bear Devlin

Hyunjin Park

James Cook

Tien Nguyen

Aaron Board

See next page for additional authors

Authors

Simon Bear Devlin, Hyunjin Park, James Cook, Tien Nguyen, Aaron Board, Christian K Bach, and Aaron S Alexander

Toward Optimal Secondary Furnace Heat Exchangers: Performance Validation of High Temperature Tube Calorimeter

Simon DEVLIN[1], Hyunjin PARK[2], James COOK[3], Tien NGUYEN[4], Aaron BOARD[5], Christian K. BACH[6], Aaron ALEXANDER[7*]

[1, 2, 3, 4, 5, 6, 7]Oklahoma State University, Mechanical and Aerospace Engineering, Stillwater, Oklahoma, USA
[1]sdevlin@okstate.edu, [2]hyunjin.park@okstate.edu, [3]james.cook10@okstate.edu, [4]tien.nguyen10@okstate.edu, [5]aaron.board@okstate.edu, [6]cbach@okstate.edu, [7, *]aaral@okstate.edu

ABSTRACT:

The growing sense of urgency surrounding carbon emissions has exacerbated the need for HVAC solutions that are energy efficient, cost-effective, and environmentally friendly. In North America, most households rely on a central furnace for heating, so serious time and effort is invested into optimizing these appliances. Currently, secondary furnace heat exchanger development teams lack the heat and mass transfer correlations necessary for accurate performance modeling, requiring costly experimental iterations and leading to suboptimal design. Furnace secondary heat exchangers operate at inlet temperatures upwards of 350°F at dew points above 100°F, increasing the difficulty reaching and replicating steady state conditions of the flue gas during calorimetric testing of individual tubes. The purpose of this project is to address these challenges through the development, construction, and testing of a calorimeter that can accurately simulate the flue gas conditions entering the secondary heat exchanger in a typical residential furnace. The system will acquire temperature and condensate mass flow rate data to perform an energy balance across the test section. The collected data will then be used to tune heat and mass transfer (HMT) correlations for a range of levels of the parameters mass flow rate, tube diameter, inlet humidity, and inlet temperature. A parallel effort has resulted in a CFD simulation pipeline that automatically configures and simulates a wide variety of additional parameter levels, increasing the level of fidelity of the data to further refine the HMT correlations. To that end, it is expected that the experimental data will serve as validation data with future work being heavily focused on CFD.

Keywords: tube calorimeter; secondary furnace heat exchanger; heat and mass transfer correlations

1. INTRODUCTION

In a North American residential home, heating and cooling typically account for 55% of the energy used according to the US Residential Energy Consumption Survey (EIA, 2015), contributing significantly to carbon emissions. The most common method of reducing cost and emissions is through furnace efficiency improvements. This is achieved by the addition of secondary furnace heat exchangers, resulting in "condensing" furnaces; an example of the internal components is shown in Figure 1. Secondary furnace heat exchangers raise the efficiency of residential furnaces from 80% (non-condensing) to greater than 90% through latent heat recovery from the flue gas. The significance of this improvement is shown by Elias et al. (2018), who estimate that upgrading household furnaces in Canada would reduce Canada's greenhouse gas emissions by 14.54 tons per household. However, these furnaces are nearly 3 times as expensive because of the increased complexity which also makes them difficult to install. They require drains because of condensate formation, further complicating the design. Several studies were completed to predict heat and mass transfer for industrial furnaces, especially those in power plants, but there is little information available for residential furnaces. Yamashita et al. (2014) investigated mini-tubes in a shell and tube heat exchanger, reporting the effect that diameter and length have on heat transfer. They showed that experimental correlations can be used to validate analytical models. However, the tubes in their research were smaller than what is utilized in North American style condensing furnaces. Nonetheless, the experimental setup of Yamashita et al. was frequently referenced in the design of this setup.

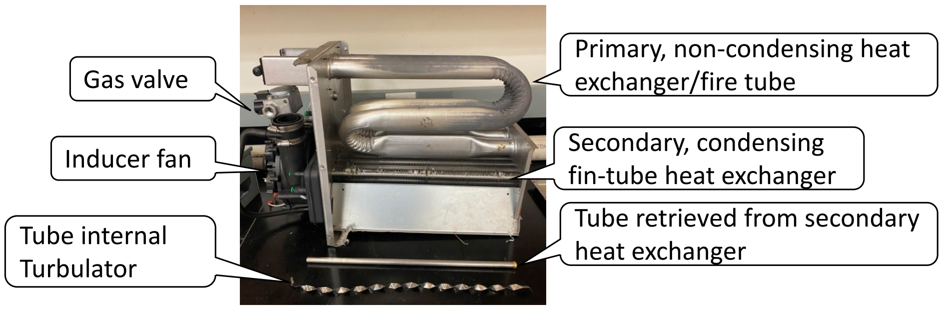

Figure 1. Picture of the internals of a high efficiency furnace with secondary heat exchanger

Currently, heat and mass transfer correlations are not available for residential furnaces. Consequentially, analytical/computational models cannot be developed and utilized. This has become a bottleneck in furnace development and hinders residential furnace design optimization. The development of analytical models would potentially allow for significant cost reduction of condensing furnaces by allowing to quickly generate more extensive simulation data for a greater range of operating conditions and designs at low cost.

This paper discusses the design and operation of a high temperature tube calorimeter experimental setup. The setup was designed to provide accurate data across a wide range of high temperatures, while maintaining versatility through the ability to easily swap calorimeter tube lengths and diameters. The thermodynamic difference between moist air and flue gas was considered negligible and therefore moist air is used to simulate the conditions of a furnace. The prescribed range of flue-side temperatures needed to accurately simulate secondary furnace heat exchanger conditions is 250° F to 350° F. Calorimeter tube diameters of interest were determined to be 3/8 in, ½ in, and 5/8 in (OD). Tube lengths to be studied range from 12 in to 24 in.

2. EXPERIMENTAL METHODS

2.1 Instrumentation

The setup, Figure 2, in flow direction of the air from the building's compressed air system, starts with a pressure regulator followed by a mass flow controller (MFC). The mass flow rate is controlled from the LabVIEW user interface using an intelligent MFC. The air is then heated by the first inline heater to approximately 130°F (dysfunctional during initial test). After that, it flows through a p-trap to prevent water from flowing back into the heater. Next the air flows into a 6 ft tall, insulated humidifier which has constant water circulation to maintain temperature uniformity. The water is heated to a range of 149-151°F. The flow at the humidifier exit is assumed to be fully saturated, which is confirmed by a dew point meter prior to further temperature or pressure changes The flow at the humidifier exit is measured by a dew point meter, a thermocouple, and a pressure gauge to determine the absolute humidity The flow is then heated by two in-line heaters placed in series to reach the designed test inlet temperature set point, which range from 250°F to 350°F. The saturated air then flows into the test section consisting of a shell and tube counterflow heat exchanger. The outer water flow is chilled in a cold-water bath to around 77°F. At the end of the test section, the condensate is collected through a mass flow meter as well as onto a scale for redundancy in condensate mass flow measurements. The exhaust air is then released into the atmosphere. Table 1 shows the location indices used in Figure 2; a process and instrumentation diagram is provided in Figure 3.

Table 1: List of components in experimental system and corresponding location

Location	Component
1	Air Intake
2	Mass-Flow controller
3	Pre-humidifier heater
4	Humidifier
5	Post-Humidifier Heaters (2)
6	Dew point meter
7	Cold-Water Bath
8	Test Section
9	Condensate flow meter & Scale

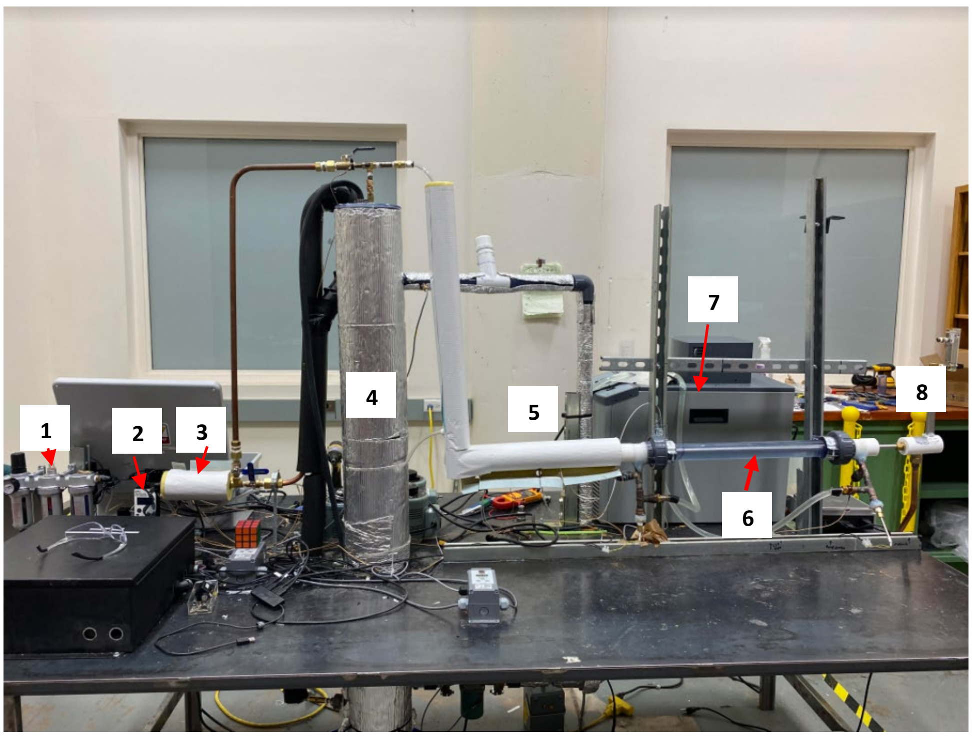

Figure 2: Experimental setup as-is, see Table 1 for component numbers/descriptions.

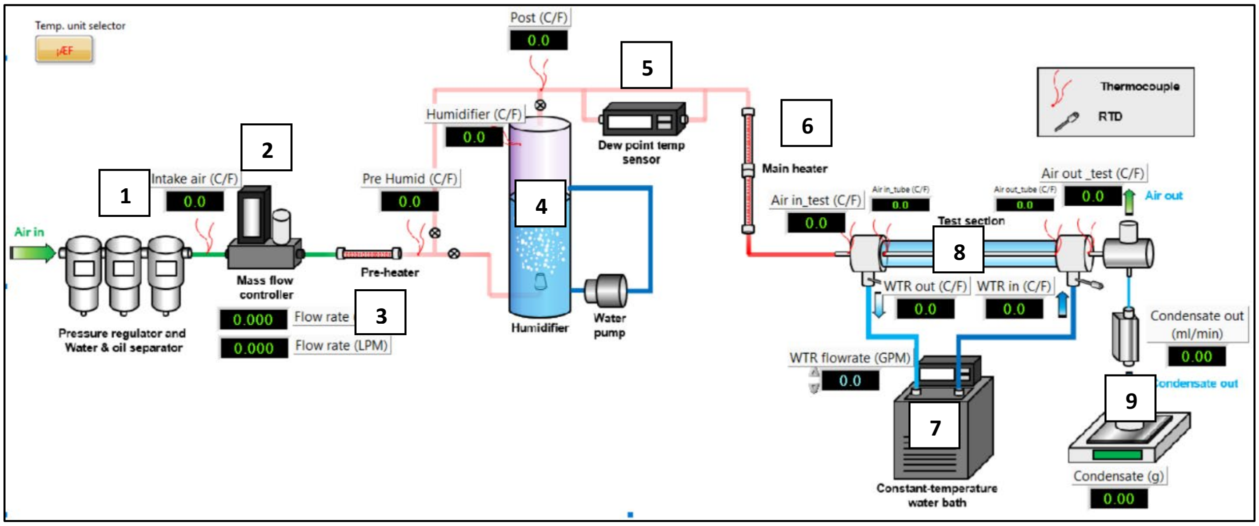

Figure 3: Schematic of experimental setup, see Table 1 for component numbers/descriptions.

The final design of the test section shown in Figures 4 and 5 consists of a stainless-steel inner tube and a clear PVC outer tube. Placed along the test section are 9 T-type thermocouples to measure the temperature gradient across the airside tube. Thermocouples are soldered to the outer surface of the stainless-steel tube and have a silicone coating to insulate them from the water. RTDs are placed in the cold-water bath flow at the inlet and exit of the shell-side of the test section to measure the water temperatures. The measurements needed for simulation validation are the temperature gradient of the air side flow, inlet and outlet temperatures of water side flow, the condensate mass flow rate, and pressure drop across the section. Through data post processing, the convection heat transfer coefficient's relations to changing flow rate, inlet temperature, tube diameter, and tube length will be determined.

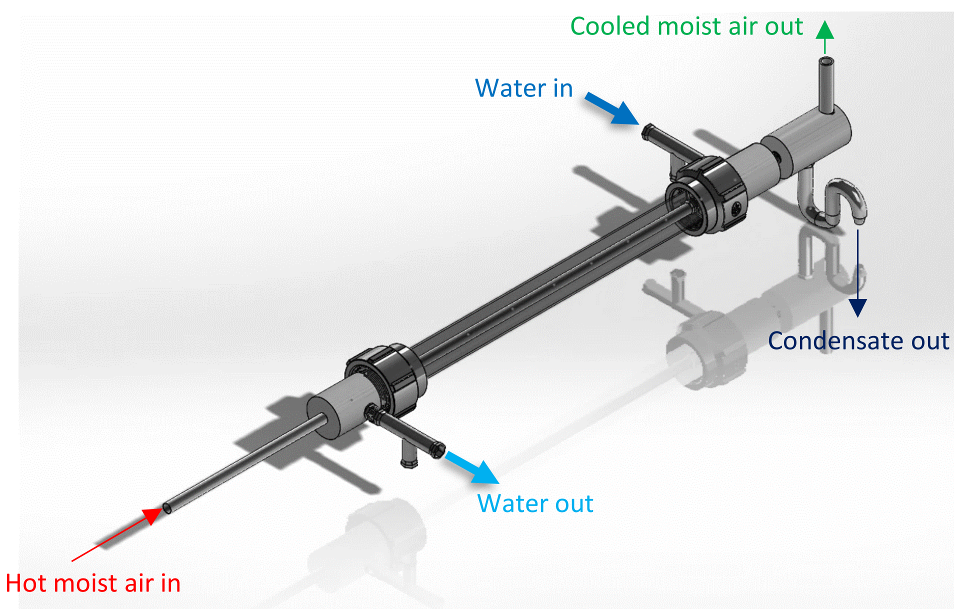

Figure 4: Rendering of test section

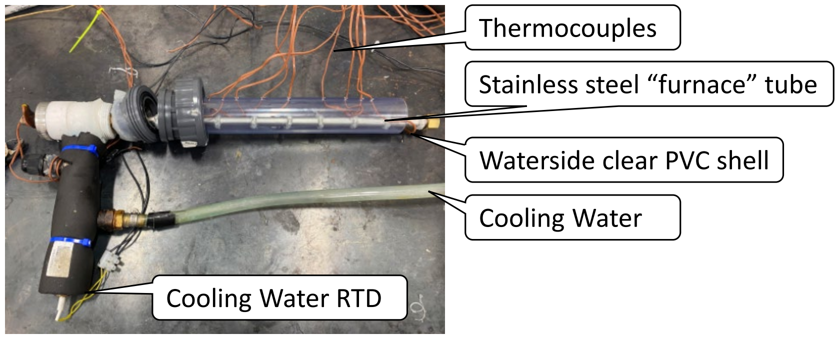

Figure 5. Installment of thermocouples across test section

2.2 Experimental Conditions

To ensure efficient experimental methods, a test plan, Table 2 was developed using the designed experimental method discussed by Czitrom (1999). The same operating conditions can then be repeated in the same manner changing diameter and tube lengths. An initial validation test was conducted using the conditions shown in Table 3.

Table 2: Temperature and flow rate conditions of experimental system

Test #	Flow Rate (CFM)	Inlet Temperature (F)
1	0.15	250
2	0.15	350
3	0.7	250
4	0.7	350

Table 3: Target and observed testing conditions

Variable	Target Testing Conditions	Observed Experimental Conditions
Test Section Inlet Temperature [°F]	346.9	347
Test Section Outlet Temperature [°F]	90	87.9
Air Mass Flow Rate [kg/s]	3.33×10^{-4}	3.31×10^{-4}
Absolute Humidity at Test Inlet	0.09069	0.0919

2.3 Uncertainty Analysis

When dealing with thermocouples as measurement instruments, it is necessary to perform an uncertainty analysis on the system. According to ASME PTC 19.1 - 1998, uncertainties consist of systematic/bias error (B) and precision/random (S) error. The equation to find the total uncertainty is shown:

$$U = \sqrt{(b_x)^2 + (s_x)^2} \qquad \text{Eq 1}$$

Systematic uncertainty can be determined by performing the uncertainty propagation using Engineering Equation Solver (Taylor Series and partial derivatives) to find the percentage of error for each instrument. Hence, it would be best to do this pre-testing or during the instrument selection phase.

The systematic or instrument uncertainty is given by Equation 2:

$$\delta R = \left\{ \left(\frac{\partial R}{\partial x_1} \delta x_1 \right)^2 + \left(\frac{\partial R}{\partial x_2} \delta x_2 \right)^2 + \cdots + \left(\frac{\partial R}{\partial x_3} \delta x_3 \right)^2 \right\}^{1/2} \qquad \text{Eq 2}$$

For temperature measurements with thermocouples, there are 4 sources of uncertainties from this system: the resolution limit of the data acquisition device, the voltage-to-temperature measurement, the reference junction (or cold junction) and random (e.g. temperature fluctuation) error.

The data acquisition method is NI 9129, which has cold junction compensation sensor of± 1°C. Type T thermocouples have a standard limit of errors of the greater of 1°C or 0.75% of the temperature reading (Omega, 2019). The hot junction is soldered onto the pipe which causes mounting inaccuracy. As suggested by ASHRAE 41.1 (ASHRAE, 2013), mounting error can be reduced by wrapping 1 inch of thermocouple wire to the tube and ensuring the curvature of the wire has the same curvature as the tube diameter.

As shown in Figure 6, the most uncertainty on the water energy balance was from the water flow meter, which was about 96%. As mentioned in the data result section, we constantly monitored and adjusted this device during testing to remain at a constant flowrate. It is recommended to replace this device in the future.

Variable±Uncertainty	Partial derivative	% of uncertainty
$\dot{Q}$ = 96.99±29.59 [W]		
$\dot{m}$ = 0.006317±0.001884 [kg/s]	$\partial\dot{Q}/\partial\dot{m}$ = 15355	95.57 %
P = 101.3±0.4137 [kPa]	$\partial\dot{Q}/\partial P$ = -0.00006898	0.00 %
T_1 = 25.06±0.1667 [C]	$\partial\dot{Q}/\partial T_1$ = 26.41	2.21 %
T_2 = 21.39±0.1667 [C]	$\partial\dot{Q}/\partial T_2$ = -26.42	2.22 %

Figure 6. *Result of the water side energy balance with percentage of uncertainty calculated*

As shown in Figure 7, the most uncertainty on the flue gas energy balance was from the dew point sensor, which was about 93%. The dry-bulb temperature at inlet and outlet was calibrated by Hyunjin Park, who oversees this project. The uncertainty from his calibration for those instruments were 0.17 K.

Variable±Uncertainty	Partial derivative	% of uncertainty
$\dot{Q}$ = 106.5±1.144 [W]		
$\dot{m}_{air}$ = 0.000331±0.000001665 [kg/s]	$\partial\dot{Q}/\partial\dot{m}_{air}$ = 165513	5.80 %
$\dot{m}_{cw}$ = 0.00002132±1.670E-08 [kg/s]	$\partial\dot{Q}/\partial\dot{m}_{cw}$ = 2.427E+06	0.13 %
P_e = 101.3±0.4137 [kPa]	$\partial\dot{Q}/\partial P_e$ = 0	0.00 %
P_{gauge} = 101.7±0.4137 [kPa]	$\partial\dot{Q}/\partial P_{gauge}$ = -0.073	0.07 %
P_i = 101.3±0.4137 [kPa]	$\partial\dot{Q}/\partial P_i$ = 0	0.00 %
T_{db} = 55.9±0.1667 [C]	$\partial\dot{Q}/\partial T_{db}$ = 0	0.00 %
T_{dew} = 51.08±3 [C]	$\partial\dot{Q}/\partial T_{dew}$ = 0.3684	93.31 %
$T_{e,db}$ = 31.05±0.1667 [C]	$\partial\dot{Q}/\partial T_{e,db}$ = -0.4383	0.41 %
$T_{i,db}$ = 175.1±0.1667 [C]	$\partial\dot{Q}/\partial T_{i,db}$ = 0.366	0.28 %

Figure 7. *Result of the flue gas side energy balance with percentage of uncertainty calculated*

Table 2: List of instruments in experimental setup

Instrument	Purpose of use	Accuracy
DPC37 Flow control	Control the air flowrate	0…30 sL/m (±0.5 RD + 0.2 FS) at calibration temperature and after tare
Liquid flow meter	Control and measure water flowrate	(0…5,000 µl µl /min, 1.5% RD) of full-scale flow
RUISHAN scale	Measure the condensing water at the outlet	0.3g
Barometer	Air pressure in the lab	0.008% of reading
Dew Point sensor	Measure the dew point temperature	−60…60°C; ±2°C

In the aforementioned test section design, there are 4 sources of uncertainties from this system: the resolution limit of the data acquisition device, the voltage-to-temperature measurement, the reference junction (or cold junction) and fluctuation error.

Temperature sensors were calibrated in-situ to eliminate systematic errors, Table 3. The reference temperature ranges from 60°F to 111°F.

Table 3: Reference and measured temperature of 8 TCs after calibration

Ref T [F]	TC1 [F]	TC2 [F]	TC3 [F]	TC4 [F]	TC5 [F]	TC6 [F]	TC7 [F]	TC8 [F]
59.0	59.0	59.5	59.6	58.7	59.5	59.2	59.2	59.3
85.8	86.0	86.5	86.4	85.6	86.4	86.0	86.1	86.2
111.9	111.4	112.0	112.2	111.5	112.1	111.3	111.9	112.0
137.6	135.4	137.3	137.6	136.9	137.4	136.3	137.2	137.4

3. CONCLUSION/FUTURE WORK

The experimental setup discussed in this paper allows for an in-depth study of heat and mass transfer and the development of the relevant correlations for secondary heat exchanger tubing of a condensing furnace. The setup was constructed, and instrumentation selected to collect data. Currently, preliminary testing is in progress, with results to be presented at the conference. After completion of the preliminary tests, data collection will begin. As data is processed, the CFD study and exiting lab data will continuously be referenced and differences in the results will be closely examined. The acquired data is expected to confirm the validity of the results of the CFD study. Subsequently, heat and mass transfer correlations will be developed, which, in turn, have the potential to allow significant increases in the efficiency and success of the design optimization of secondary furnace heat exchangers.

NOMENCLATURE

b	Bias or systematic error	R	Instrument uncertainty
$\dot{m}$	Mass flowrate	s	Random or precision error
P	Pressure or Atmospheric pressure	T	Temperature
$\dot{Q}$	Heat transfer rate	U	Total Uncertainty

Subscripts

air	Air	*g*	Gauge
cw	Chilled water	*i*	Inlet
db	Dry bulb	*x*	Generic placeholder
dew	Dew point	*1, 2, 3*	Location index
e	Exit		

REFERENCES

ASHRAE (2013). ANSI/ASHRAE Standard 41.1-2013: Standard Method for Temperature Measurement. *ASHRAE*, Atlanta, GA.

Czitrom, V. (1999). One-Factor-at-a-Time Versus Designed Experiments. *The American Statistician, 6(2).* 126-131

Elias, R. S., Yuan, M., Wahab, M. I. M., Patel, N. (2018). Quantifying saving and carbon emissions reduction by upgrading residential furnaces in Canada. *Journal of Cleaner Production, 211.* 1453-1462.

Yamashita, J. Utaka, Y. (2014). Improved performance of secondary heat exchanger for latent heat recovery from flue gas using mini-tubes. *Applied Thermal Engineering*, *67*. 230 – 239.

Omega (2019). Thermocouple types. Retrieved from https://www.omega.com/en-us/resources/thermocouple-types on 06/13/2022.

EIA (2015a). Residential Energy Consumption Survey (RECS). Table CE3.1 End-use consumption in the U.S. - totals and averages 2015. *US DOE Energy Information Administration.* Washington, DC.

ACKNOWLEDGEMENT

The authors of this paper would like to thank Dr. Roy Crawford and Dr. Tao Geng at Johnson Controls, Inc. for their continued support. This senior design project was funded by the Oklahoma State University's Center for Integrated Building Systems (CIBS).